NANO LETTERS

2007
Vol. 7, No. 5
1208−1212

Where, and How, Does a Nanowire Break?

Dongxu Wang, Jianwei Zhao,* Shi Hu, Xing Yin, Shuai Liang, Yunhong Liu, and Shengyuan Deng

School of Chemistry and Chemical Engineering, Nanjing University, Nanjing, China 210008

Received December 14, 2006; Revised Manuscript Received February 26, 2007

ABSTRACT

Using molecular dynamics (MD) simulation, we studied the structural transformation and breaking mechanism of a single crystalline copper nanowire under continuous strain. At a certain strain rate, an ensemble of relaxed initial states of the nanowire can preferentially go through one or more paths of deformation. In each deformation path, disordered atoms can be generated at the specific positions of the nanowire, where necking and breaking take place afterward. Such a breaking position is not predetermined; multiple initial states lead to a strain-rate-dependent, statistical distribution of breaking positions.

Nanoscale, defect-free materials like nanowires are of great interest due to their potential applications in micromechanical and electronic systems (MEMS), molecular electronic devices, and other fields of nanotechnology. During the past decade, a great deal of effort has been made to elucidate the structural and mechanical properties of nanowires. A number of studies focused on the problem of nanowire breaking, but a comprehensive understanding has not yet been achieved. Ikeda et al.[1] discovered that, under sufficiently high strain rate (∼5% ps^{-1}) at 300 K, Ni nanowire is elastic up to 7.5% strain, after which the continuous strain induces a transition from the crystalline phase to the amorphous phase. Koh et al.[2] found that, for Pt nanowires at 300 K, the critical strain rate to induce a complete amorphous deformation is 4.0% ps^{-1}, while the onset of amorphization occurred at a lower strain rate, 0.4% ps^{-1}. Amorphous nanowires recrystallize when the strain rate was slowed down.[1,3] For lower strain rate, dislocation and relaxation steps repeat.[2,4] During this repeated process, global crystalline order changed to local close-packed atomic arrangements,[5] and the nanowire's surface reconstructed.[6] Various disorders, faults, and vacancies were then created in the nanowires, and they played an important role in nanowire elongation and breaking.[5−9] Radial distribution functions (RDF) and stress−strain relationships characterize these different deformation mechanisms. The deformation mechanism also depends on nanowire's size, shape, surface orientation, etc, as well as strain rate.[9,10] Experimentally, a nanowire can form at nanocontacts, and necking phenomenon can be observed.[11,12]

Although much progress has been made, the study of nanoscale objects can still lead to new findings, which may be governed by the microscopic statistics. A typical problem is: where does a finite-length nanowire break under tension? This has not been answered yet. One might intuitively think that a nanowire would break at its middle along the strain direction if both the wire and the tension are symmetrical. Yet according to a number of atomic configuration plots,[2,3,7] there is no evidence that breaking always takes place at the middle. These plots suggest that there is a probability for a nanowire to break at a certain position. As nanowires can deform by different mechanisms,[13] such tendencies may be correlated with the mechanism that come into play with different strain rates.

It is not easy to find such a probability distribution. The common "strain-and-relax" method used in simulation of a nanowire under tension makes the study of breaking position difficult. In this model,[1−3,8] strain is exerted at a certain time, and then the nanowire relaxes to a new equilibrium state before strain is exerted again. This quasi-equilibrium method ignores the difference in the initial states, which would greatly influence the final atomic configuration due to the characteristics of many-body problems. In a dynamic, continuous pulling method,[7,14] the nanowire is strained from a certain equilibrium state and evolves to a final atomic configuration. Strain from another equilibrium state can lead to a different final atomic configuration. If strain is exerted on an ensemble of equilibrium states, the evolution of the whole ensemble can be revealed. This will yield the distribution of breaking positions for a nanowire at certain conditions.

To address the question about breaking, we performed molecular dynamics simulations of nanowires strained by continuous pulling. Single crystalline copper nanowires (Figure 1), positioned with {100} surfaces facing out, are

* Corresponding author. E-mail: zhaojw@nju.edu.cn.

10.1021/nl0629512 CCC: $37.00
Published on Web 03/28/2007

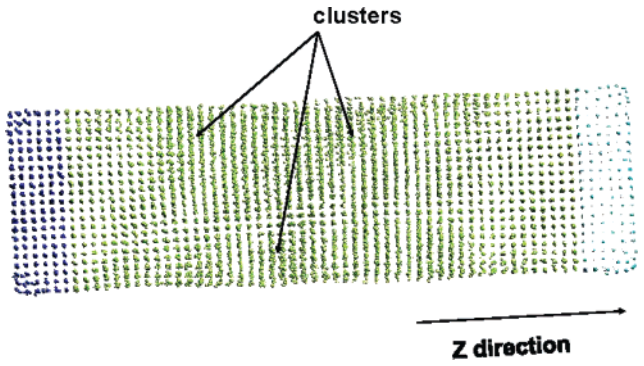

Figure 1. Atomic configurations of the nanowire at 153 ps for 0.13% ps^{-1} strain rate, when clusters already appear. Before clusters appear, nanowires of different initial states look the same. The wire's size is $10.5a \times 10.5a \times 30.5a$ (x, y, z direction, respectively, and a is copper lattice constant 0.362 nm) with a total atom number 13 451 for 1.3 and 0.13% ps^{-1} rates and is smaller, $8.5a \times 8.5a \times 24.5a$ with totally 7081 atoms, to expedite the simulation for 0.016% ps^{-1} rate. Half lattice is included so that the wire is completely symmetric in all three directions. Two ends (three lattice spacing thick, free during relaxation but fixed in the $x-y$ plane after strain is applied) of nanowires along z-direction are pulled at constant speeds of 72, 7.2, and 0.72 ms^{-1}, corresponding to strain rates of 1.3, 0.13, and 0.016% ps^{-1}, respectively. All atoms are first positioned on ideal Cu crystalline lattices. For samples under 1.3 and 0.13%/ps strain, the Nth sample will have experienced $102 + 1.02N$ ps of relaxation before tension is applied. For samples under 0.016%/ps strain, the Nth sample will have experienced $5.1 + 1.02N$ ps of relaxation before tension is applied. In either case, the first 102 or 5.1 ps will give the sample enough time to reach an equilibrium state (see Figure 3).

under three rates of strain, 1.3, 0.13, and 0.016% ps^{-1}, respectively. These three strain rates are representative for two orders of magnitudes; they can give the typical nanowire deformation mechanisms and breaking position distributions as we will detail below. Free boundaries are used.[6] Embedded-atom method (EAM) was used for potential calculation, and the EAM potential form and parameters were taken from the analytical nearest-neighbor model proposed by Johnson,[15,16] which successfully describes the properties of FCC metal. With a constant temperature 293 K, the leapfrog method with time step 5.1 fs was used for integrating the equation of motion. The strain begins at statistically independent different states of one ensemble (see Supporting Information). Energy and stress are recorded at every step, and the atomic configuration plots are saved as snapshots. The breaking positions for all the simulations of each strain rate are evaluated by using an atom number ratio (ANR) defined as

$$\text{ANR} = \text{atom number in the smaller part after breaking/total atom number of the nanowire} \times 100\%$$

ANR can be used here to indicate the position the nanowire breaks.

A simple statistical analysis of the simulation results for each strain rate gives distinct ANR distributions (Figure 2). At the strain rate of 1.3% ps^{-1}, the nanowire is very likely to break symmetrically, with most probable ANR values between 40 and 50%. At the intermediate strain rate 0.13% ps^{-1}, the nanowire tends to be broken asymmetrically, with

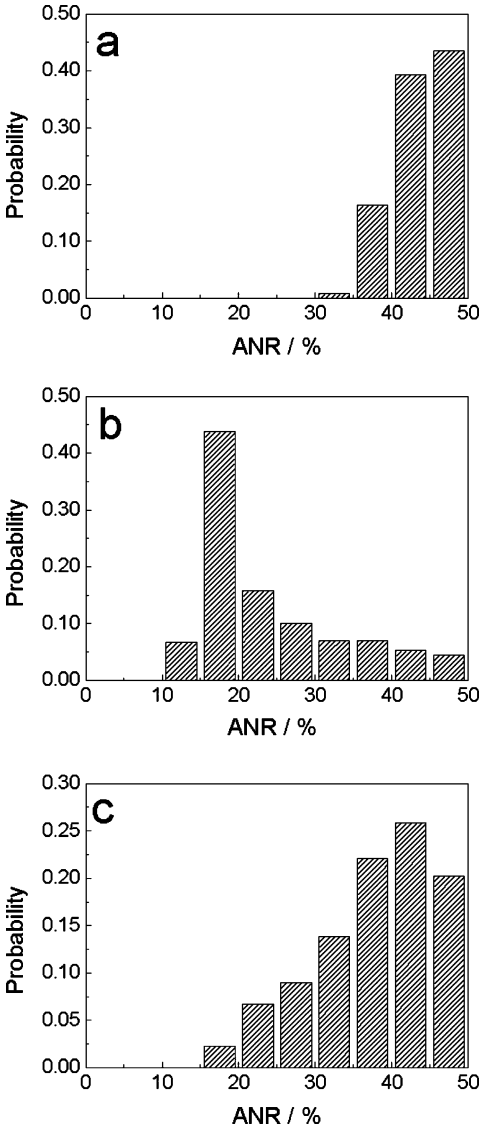

Figure 2. ANR distributions at (a) 1.3% ps^{-1} strain rate, (b) 0.13% ps^{-1} strain rate, and (c) 0.016% ps^{-1} strain rate.

most probable ANR values around 15−20%. The low strain rate 0.016% ps^{-1} shows a high probability of ANR 40−45%, i.e., breaking with high symmetry.

Because different strain rates can generate different orders of atomic arrangement,[9] i.e., different symmetry, we consider both breaking symmetry and atomic arrangement in our study as the results of different deformation mechanisms under different strain rates. We therefore investigated the evolution of the atomic arrangement, potential energy, and stress−strain relationship to explore these causal relationships. Because 300 samples are available for each strain rate, we discuss the most prominent features, i.e., the features that appear in all or most atomic configurations, potential energy curves, and stress−strain relationships.

For all strain rates, there is a sudden drop in both the potential energy and stress−strain relations after they increase to a limit. This indicates a significant structural phase transition. The atomic configuration pictures at this moment show clusters present in the middle part of wire. This offers a physical interpretation. Under a continuous strain, atoms

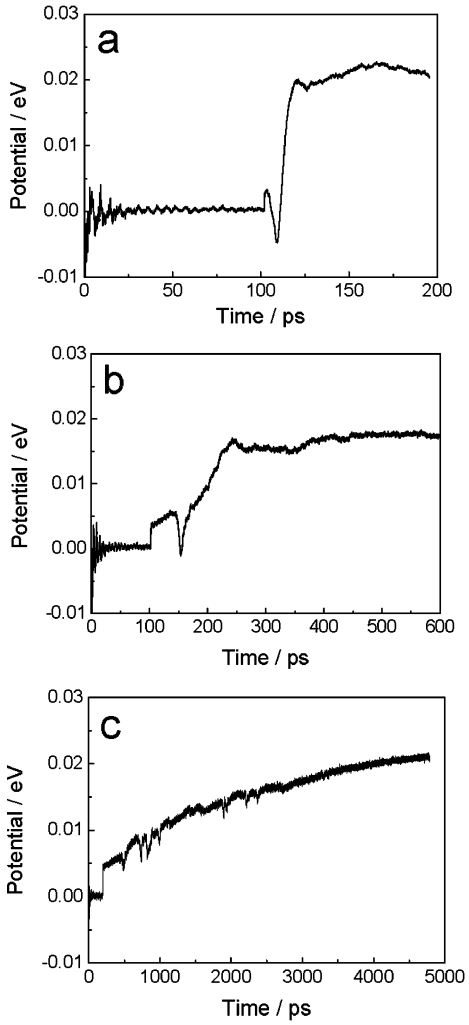

Figure 3. Typical potential curves at (a) 1.3% ps^{-1} strain rate, (b) 0.13% ps^{-1} strain rate, and (c) 0.01625% ps^{-1} strain rate, respectively. Strain begins at 102 ps for (a) and (b), and at 51 ps for (c). Equilibrium potential is set to zero.

cannot always retain their relative positions at ideal crystalline lattices, so they collapse after the strain reaches a limit. Four to six atoms collapse into a small cluster to reduce the stress. Many such clusters appear in the middle region of the wire. Both short-range and long-range orders in this region are lost. The radial distribution function (RDF) analysis confirms this (see Supporting Information). The higher the strain rate, the more clusters appear. These local clusters had been noted in previous studies.[5,9,14,17] Subsequent deformation mechanisms differ depending on strain rate.

For strain rate of 1.3% ps^{-1}, the plot (see inset of Figure 4a) shows that the clusters in the middle part of the nanowire soon changed to an amorphous configuration. Necking takes place at these amorphous positions, and the wire is elongated superplastically. The corresponding potential energy arises after the above-mentioned sudden drop until it reaches a plateau (Figure 3a). The stress−strain curve decreases after that sudden drop. This process is consistent with the reported high strain rate simulation of nanowires by Chen et al.[18] and Ikeda et al.[1]

At the strain rate of 0.13% ps^{-1}, configuration snapshots (inset of Figure 4b) show a different deformation mechanism.

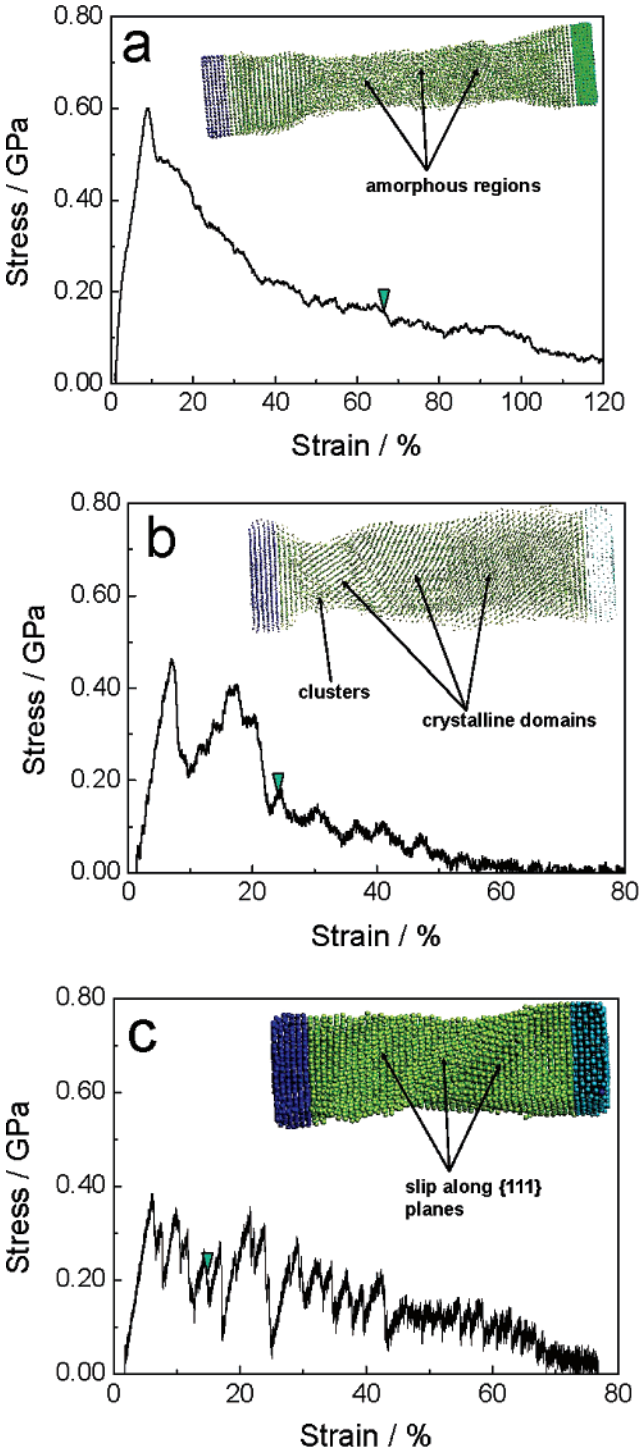

Figure 4. Typical stress−strain relationships at (a) 1.3% ps^{-1} strain rate, (b) 0.13% ps^{-1} strain rate, and (c) 0.016% ps^{-1} strain rate, respectively. Insets are atomic configurations at the necking stage: (a) at 153 ps for 1.3% ps^{-1}, (b) at 301 ps for 0.13% ps^{-1} strain rate, and (c) at 1020 ps for 0.016% ps^{-1} strain rate. The green triangle on the stress−strain curve indicates the stage when the atomic configuration snapshot is shown. Atoms in inset of (c) are drawn larger so that the slip can be more clearly seen.

The clusters traverse from the middle part to the two ends in ∼50 ps in a wavelike manner. Necking then takes place preferentially near one end, where the clusters are, by the slip of crystalline domains around these clusters. An atom-thick neck similar to previously reported ones[2,19] is also

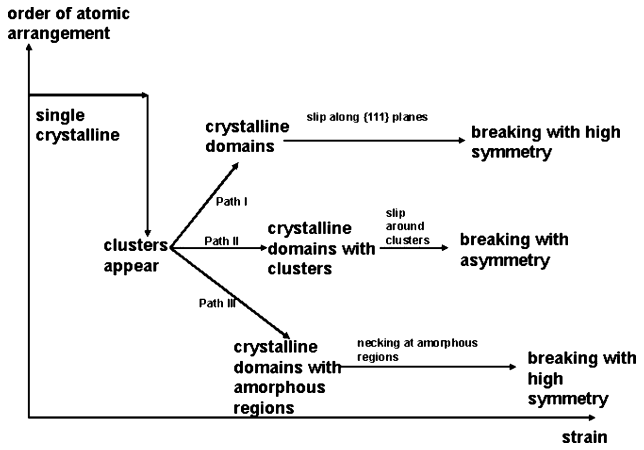

Figure 5. Complete deformation paths.

observed at the final stage just before breaking (See Supporting Information). The middle area where clusters initially formed has recrystallized to differently oriented domains. The RDF (see Supporting Information) reflects the changes of short-range and long-range order during this process. For this strain rate, the potential energy is shown in Figure 3b, similar to that for the strain rate of 1.3% ps^{-1}. The stress−strain curve (Figure 4b) has one peak at ∼7.5% strain, followed by a lower second peak and then a decrease.

The structural transformation at a low strain rate of 0.016% ps^{-1} (inset of Figure 4c) proceeds through a third mechanism that differs from the other two just described. Under this condition, small numbers of clusters appear but soon revert to crystalline domains. This deformation process is just as reported before:[2,4] the atomic arrangement deviates from the global minimum and then is stabilized in a local minimum. This process repeats many times during the elongation process. Crystalline domains slip on a number of close-packed {111} planes until breaking at one slipping layer near the middle part. The potential curve has many drops, in agreement with the appearance of the above-mentioned recurring structural stages.

Now we come to a hypothetical conclusion. We propose a full process that different strain rates induce different paths of structural transformations, generate different local disorders, and yield different probability distributions of breaking position. Figure 5 summarizes this hypothesis, which is in large agreement with that proposed by Koh and co-workers.[13] Local disorder in the form of amorphous regions or clusters, and their boundaries with crystalline domains, are weak places where nanowires tend to neck and break. Under strain, clusters are first generated in the middle region to release the high stress when strain reaches a limiting value; that is the first structural transformation. These clusters have a tendency to traverse several times in a wavelike manner and gradually recrystallize; the time scale for this process is about 100 ps for the present wire length, according to the potential curve for the strain rate of 0.016%/ps. Further strain may interrupt this process: During ∼100 ps, a 1.3% ps^{-1} strain rate would generate ∼130% strain, while a 0.016% ps^{-1} rate generates only a ∼1.3% strain. Compared with the elastic strain limit of ∼7.5%, these different strain rates will result in different deformations. Under a high strain rate, e.g., ∼1.3% ps^{-1}, (along path I), these clusters are "trapped" in the middle part before they can traverse to other places. These clusters transform to an amorphous phase, and this amorphous area then turns thinner as strain becomes larger, until beaking. Superplasticity can be observed in this situation. The wire then breaks with highest probability at the middle part of the wire, i.e., with ANR of 40−50%. For intermediate strain rate, e.g., ∼0.13% ps^{-1}, (along path II), the clusters can traverse toward two ends of the wire, with the middle part reverting to crystalline domains. A number of clusters are very likely to be localized near two ends, at ∼15−20% position under 0.13% ps^{-1} strain rate for present study. Here we should point out that, for nanowires of different length, this position should vary. Crystalline domains slip around these small clusters. Then necking appears at this position by the sliding along interfaces between crystalline and amorphous domains. The nanowire is elongated, and then the neck turns thinner till separation. So the nanowire is more likely to break near two ends, i.e., with asymmetry. For low strain rate of 0.016% ps^{-1} (along path III), the small number of clusters initially generated in the middle part has sufficient time to traverse and recrystallize before necking takes place. At this strain rate, the wire is elongated by slipping of crystalline domains along many {111} planes. The nanowire maintains high symmetry along its length; the most probable breaking position is near the middle part, in other words, it tends to break with symmetry.

It should be noted that there might not be critical strain rates to distinguish the three paths of deformations. For the three strain rates in present study, 1.3, 0.13, and 0.016% ps^{-1}, the three paths of deformation mentioned above are representative. However, it is highly probable that, at a specified strain rate, a nanowire can go through mixed paths rather than a single path. We simulated the tension and breaking of the nanowire under a strain rate of 0.041% ps^{-1} (a value between 0.13 and 0.016% ps^{-1}) and found that the wire is likely to break at both 15−20% and 45−50% positions (See Supporting Information). The atomic configuration plots show that some of the samples at this strain rate take path II, while others take path III. This further implies that an ensemble of initial states would evolve along different paths with characteristic probabilities.

In summary, we performed molecular dynamics simulations of nanowires in tension using a dynamic, continuous pulling method. The results of nanowire deformation are in close agreement with those reported for the "strain-and-relax" method. At different strain rates, the nanowire takes different paths of deformation with different probabilities because the order of atomic rearrangement is dependent on strain rate. For each of the paths, there exists a statistical distribution of the nanowire breaking positions. Such a probability distribution should reflect the difference in initial equilibrium states in which thermal fluctuations play a role. It would thus be valuable for future studies to explore how temperature can shift the breaking position probability distribution. Further, as pointed out by Sørensen et al.,[9] deformation mechanisms are also dependent on the size, shape, and crystal

orientation of a nanowire. Their impacts on the probability distribution of the breaking position are worth studying as well.

Acknowledgment. This project was partially supported by the National Natural Science Foundation of China (nos. 20435010, 20503012), National Natural Science Funds for Creative Research Groups (20521503), and the Natural Science Foundation of Jiangsu Province (BK2005413). We thank Dr. Meyer Jackson for comments on the manuscript.

Supporting Information Available: Plots and animations. This material is available free of charge via the Internet at http://pubs.acs.org.

References

(1) Ikeda, H.; Qi, Y.; Çagin, T.; Smawer, K.; Johnson, W. L.; Goddard, W. A., III. *Phys. Rev. Lett.* **1999**, *82*, 2900.
(2) Koh, S. J. A.; Lee, H. P.; Lu, C.; Cheng, Q. H. *Phys. Rev. B* **2005**, *72*, 085414.
(3) Branício, P. S.; Rino, J.-P. *Phys. Rev. B* **2000**, *62*, 16950.
(4) Mehrez, H.; Ciraci, S. *Phys. Rev. B* **1997**, *56*, 12632.
(5) Wen, Y.-H.; Zhu, Z.-Z.; Shao, G.-F.; Zhu, R.-Z. *Physica E* **2005**, *27*, 113.
(6) Diao, J.; Gall, K.; Dunn, M. L. *J. Mech. Phys. Solids* **2004**, *52*, 1935.
(7) Komanduri, R.; Chandrasekaran, N.; Raff, L. M. *Int. J. Mech. Sci.* **2001**, *43*, 2237.
(8) Wu, H. A. *Euro. J. Mech. A* **2006**, *25*, 370.
(9) Sørensen, M. R.; Brandbyge, M.; Jacobsen, K. W. *Phys. Rev. B* **1998**, *57*, 3283.
(10) Zhang, H. Y.; Gu, X.; Zhang, X. H.; Ye, X.; Gong, X. G. *Phys. Lett. A* **2004**, *331*, 332.
(11) Gai, Z.; Li, X.; Gao, B.; Zhao, R. G.; Yang, W. S.; Frenken, J. W. M. *Phys. Rev. B* **1998**, *58*, 2185.
(12) Halbritter, A.; Csonka, Sz.; Kolesnychenko, O. Y.; Mihály, G.; Shklyarevskii, O. I.; van Kempen, H. *Phys. Rev. B* **2002**, *65*, 045413.
(13) Koh, S. J. A.; Lee, H. P. *Nanotechnology* **2006**, *17*, 3451.
(14) Komanduri, R.; Chandrasekaran, N.; Raff, L. M. *Mater. Sci. Eng. A* **2003**, *340*, 58.
(15) Johnson, R. A. *Phys. Rev. B* **1988**, *37*, 6121.
(16) Johnson, R. A. *Phys. Rev. B* **1988**, *38*, 3924.
(17) Ju, S.-P.; Lin, J.-S.; Lee, W.- J. *Nanotechnology* **2004**, *15*, 1221.
(18) Chen, D.-L.; Chen, T.-C. *Nanotechnology* **2005**, *16*, 2972.
(19) da Silva, E. Z.; da Silva, A. J. R.; Fazzio, A. *Phys. Rev. Lett.* **2001**, *87*, 256102.

NL0629512